Korean J. Chem. Eng., 38(7), 1308-1316 (2021)
DOI: 10.1007/s11814-021-0794-4

pISSN: 0256-1115
eISSN: 1975-7220

INVITED REVIEW PAPER

Radical-driven photocatalytic transformation of organic molecules

Minsoo Kim, Gui-Min Kim, Nianfang Wang, and Doh C. Lee†

Department of Chemical and Biomolecular Engineering, Korea Advanced Institute of Science and Technology (KAIST), Daejeon 34141, Korea

(*Received 5 January 2021 • Revised 19 March 2021 • Accepted 28 March 2021*)

Abstract−In photocatalysis, photons are absorbed by semiconductor materials and photogenerated electrons and holes migrate to the catalytic surface for desired reactions. Photocatalytic reduction and oxidation of organic molecules pose significant challenges and opportunities, with the surging demand for energy-efficient and carbon-neutral organic synthesis. In this review, we highlight the recent progress in the expanding area of radical-driven photocatalytic transformation of organic molecules. Our focus expands from heterogeneous catalysts to quantum dots, summarizing the reaction mechanism and photocatalytic activity, in reference to conventional molecular catalysts.

Keywords: Photocatalysis, Semiconductor Materials, Organic Transformations, Reactive Radical Species, Quantum Dots

INTRODUCTION

Since the seminal water-photolysis study by Honda and Fujishima in 1972, the ever-growing field of photocatalysis has been in pursuit of the *Holy Grail* of carbon-neutral energy production and fine-chemical synthesis [1]. Significant amount of progress has since been reported in the photocatalytic reactions of hydrogen production [2-9], CO_2 reduction [10-14], and environmental purification [15-17]. Because of the implications of these reactions in the context of global energy challenges, photocatalysis has rightfully drawn a great deal of interest. Yet, the quest for ultra-high-efficiency photocatalysts has remained far from complete, particularly because of relatively low reactivity of transformation of organic molecules. Organic transformations, such as carbon-hydrogen (C-H) arylation [18] and the Diels-Alder reaction [19,20], typically involve molecular catalysts such as Ru-based or Ir-based complexes. While the molecular catalysts record relatively high laboratory-scale efficiency, the noble metal-based molecular catalysis poses cost and recycling issues. For this reason, the field has turned to semiconductor nanoparticle photocatalysts for organic transformation.

Two research thrusts have represented the field of semiconductor photocatalysts for organic transformations: heterogeneous photocatalysts and quantum dots (QDs). Because heterogeneous photocatalysts form poor dispersion in solution, organic reactions occur at the interface between two or more phases. The crucial advantage of heterogeneous photocatalysis is the favorable recycling after the reaction [21,22]. Besides, heterogeneous photocatalysts are usually inexpensive and mild [23], and even easy to synthesize [24,25]. QD-based catalysts have recently been studied in an effort of finding an alternative to molecular catalysts [26,27]. QDs have been utilized for light-emitting devices [28,29] or photocatalytic applications [30,31]. Their unique properties, such as size-tunable energy levels [32] and the large extinction coefficient, make them attractive as high-absorption photocatalyst materials in which relatively small catalyst loading is desired [26]. Surface ligand exchange process turns QDs soluble in various solutions, leading to well-controlled surface polarity of the nanoparticles (NPs) [33,34].

In contrast to conventional photocatalysis such as H_2 production or CO_2 reduction, oxidation reaction is the key in most cases of organic transformation mediated by semiconductor photocatalysts [35,36]. Consequently, valence band potential and the behavior of photo-generated holes became more important. Carbon radical intermediates can be formed via oxidation reaction, and they usually drive the organic reaction to produce valuable products. On this account, it is of utmost importance to investigate reaction pathways and to search for solvents that stabilize radical species.

In this review, we highlight the progress in photocatalysis in the comparative context of semiconductor particles and molecular catalysts for radical-drive organic transformations. The discussion includes the classification of various reactions, according to bond formation, bond cleavage, and oxidation. Furthermore, characteristics and merits of each photocatalyst are organized. The importance of oxidation reaction and its radical chemistry are also emphasized.

PHOTOCATALYSIS FOR ORGANIC TRANSFORMATIONS BY SEMICONDUCTOR MATERIALS

Despite the immense variety of organic transformations, or because of the seemingly unbounded diversity, we review recent progress based on the enumerated sections: bond formation, bond cleavage, and oxidation reaction.

1. Bond Formation Reaction

C-C bond formation reaction has been regarded as an essential tool for pharmaceutical application and organic synthesis among various bond formation reactions [37,38]. This coupling reaction is usually induced by transition metal based molecular catalysts, such as palladium or ruthenium, and has been studied extensively

†To whom correspondence should be addressed.
E-mail: dclee@kaist.edu

for a long time [39]. In photocatalysis by semiconductor materials, many of QD-based photocatalysts are known for their ability to catalyze the bond formation reaction, C-C bond in particular [26,27]. Plenty of reactions are classified as C-C coupling [40], cycloaddition [41], and polymerization [42] according to the number of C-C bond formation as one, two and more, respectively. The brief interpretations and research trends of each catalyst are also mentioned together.

1-1. Carbon-carbon Coupling Reaction

Exclusively, titanium dioxide (TiO_2) has recorded good photocatalytic activity in heterogeneous photocatalysis. This is because TiO_2 has wide band gap (P25, 3.2 eV) to absorb ultraviolet light [43] and deep valence band potential (2.7 eV, vs. NHE) to efficiently form hydroxyl radicals (OH·) and superoxide radicals (O_2^{-}) [44]. Consequently, it is specialized for photocatalysis such as water purification and dye degradation [45]. There are many advantages in TiO_2 photocatalysis, including price competitiveness or innocuousness, even can be used as nanomaterial in cosmetics [46]. Though, diverse C-C coupling reactions with TiO_2 have been reported continuously, C-H arylation reaction was performed first [40]. Zoller discovered that there is an unexpected role of TiO_2 that can develop the direct arylation of heteroaromatic compounds as shown in Fig. 1(a). High yield was evaluated for five cycles even after recycling (88-93%) by easy separation. Moreover, dual role of TiO_2 was established not only catalyzing azoether formation but also as the reaction initiator.

In QD-based catalysis, cadmium chalcogenide photocatalysts were studied first for C-C coupling reaction, via ligand engineering. Previously, cadmium sulfide (CdS) photocatalyst was mostly used for environmental and energy application [47,48]. But recently, the utilization of CdS has emerged for organic synthesis because its band energy level is appropriate enough to oxidize organic molecules [51-53]. Especially, it has suitable band potential to produce superoxide radicals and carbon radicals by direct oxidation. Even CdS QDs have moderate direct band gap (bulk, 2.25 eV) to absorb visible light, as well as tunable band potential [52,53]. In addition to photoreforming of various materials, photoredox α-vinylation was also catalyzed with CdS QDs [26]. Previous study about direct C-H vinylation cycle between α-amino acids N-aryl amines was driven by Ir-based molecular photocatalysts [54]. However, the original coupling protocol requires high cost Ir-based catalysts. In later study described in Fig. 1(b), CdS QDs replaced Ir-based molecular catalysts successfully. Utilizing unique advantages of QDs, ligand engineering was derived. The change of ligands from native oleate to octyl phosphonate/oleate mixed monolayer induced increasing the initial rate of the reaction by a factor of 2.3. They interpreted that this phenomenon is caused by the increased permeability of the ligand shell of the QDs, lowering the kinetic barrier for the rate-limiting step. The rate-limiting step was oxidation of phenyl trans-styryl sulfone, which was confirmed by the method of initial rates.

Another cadmium chalcogenide material, cadmium selenide (CdSe) also approved its ability as catalyst of various C-C coupling reactions. CdSe has been expected as promising material, varying its shape to QDs, nanorods (NRs) [55], and even nanoplatelets (NPLs) [56,57]. Particularly, CdSe QDs usually have narrow band gap energy (bulk, 1.7 eV) [52] and their heterostructures are often preferred for efficient photocatalysis [61-63]. The first C-C bond forming reactions with CdSe QDs photocatalysis were indicated by Caputo et al [27]. This article incorporates five reactions (β-alkylation, β-aminoalkylation, dehalogenation, amine arylation, and decarboxylative radical formation) and every scheme is similar to Fig. 1(c). As against Ru-based or Ir-based molecular photocatalysts, low catalyst loadings were highlighted once more and higher turnover numbers and frequencies were shown. This can be another successful example of substitution of molecular catalysts.

Though, cadmium-based photocatalysts have scalability matter

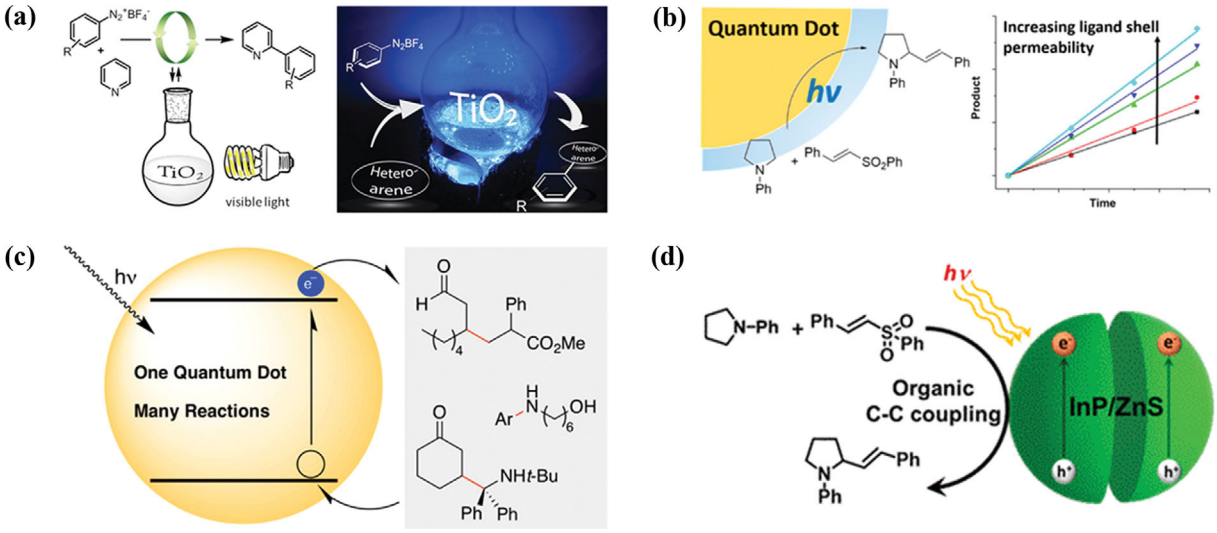

Fig. 1. (a) Catalytic scheme of C-C coupling reactions by TiO_2. Reproduced with permission from [40]. Copyright (2015) American Chemical Society. (b) Reaction scheme and production rate graph of C-C coupling reactions by CdS QDs. Reproduced with permission from [26]. Copyright (2017) American Chemical Society. (c) Schematic concept of C-C coupling reactions by CdSe QDs. Reproduced with permission from [27]. Copyright (2017) American Chemical Society. (d) Overall scheme of C-C coupling reactions by InP/ZnS QDs. Reproduced with permission from [61]. Copyright (2019) American Chemical Society.

caused by heavy-metal use. Besides, an analogous study of C-C coupling reaction with InP/ZnS was also announced [61] and its concept is shown in Fig. 1(d). Because of the low stability of InP cores [62,63], core/shell heterostructure is often designed for various applications [64,65]. Though the main reaction and its mechanism are the same as previous study with CdS QDs [26], this research has the major merit of heavy-metal-free process. At first, Chakraborty et al. observed photocatalytic reduction ability of InP/ZnS by ferricyanide reduction experiments to ferrocyanide. Myristic acid (MA) functionalized InP/ZnS QDs were synthesized first as reported procedure [66], and anionic 11-mercaptoundecanoic acid (MUA[-]) ligand replaced them by exchange protocol. Consequently, a high photoconversion yield of ~70% was exhibited even though their concentration of catalysts was only about 600 nM. Moreover, the recyclability aspect was discussed, which is one of the challenges in QD-based photocatalysis. QDs-coated Whatman-60 filter paper facilitated the reuse of catalysts even for five times. Eventually, C-C bond formation between 1-phenyl pyrrolidine (PhPyr) and phenyl-trans-styryl sulfone ($PhSO_2$) was derived with appreciable photoconversion yield of ~52%.

1-2. Cycloaddition Reaction

Cycloaddition reaction is also an integral versatile tool in organic synthesis, and its stereochemistry and electronic coherence of substituted groups are frequently studied [67,68]. During the reaction, two C-C bonds are newly formed, making a new ring structure. In photocatalysis by semiconductor materials, graphitic carbon nitride ($g\text{-}C_3N_4$) was reported firstly as an efficient semiconductor photocatalyst for cycloaddition. It is a polymeric material synthesized by simple thermal polymerization of various precursors (urea, melamine, and cyanamide) [69,70], and has high thermal and chemical stability [71]. Originally, $g\text{-}C_3N_4$ is an effective heterogeneous photocatalyst in extensive fields. Water splitting to produce hydro-

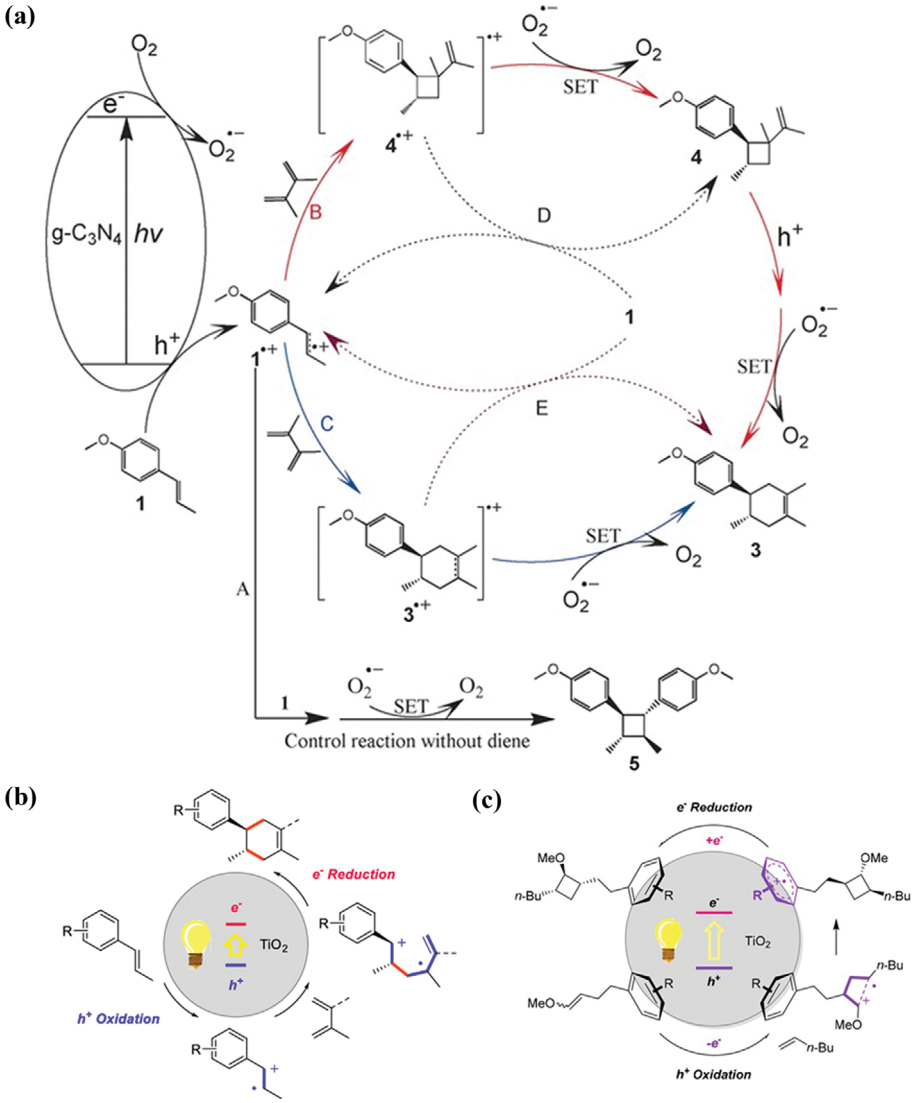

Fig. 2. (a) Schematic mechanism of [4+2] cycloaddition with $g\text{-}C_3N_4$ [41]. John Wiley & Sons. © 2017 WILEY-VCH Verlag GmbH & Co. KGaA, Weinheim. (b) [4+2] cycloaddition reaction cycle with TiO_2. Reproduced from [76]. Copyright (2019) American Chemical Society. (c) Two pathways of [2+2] cycloaddition reaction with TiO_2. Reproduced with permission from [97]. Copyright (2018) American Chemical Society.

gen [75,76], and mineralization [74] are the representative examples. Zhao et al. demonstrated photocatalytic [4+2] cycloaddition using carbon nitride, called as Diels-Alder reaction [41]. Remarkable apparent quantum yield (AQY) reached 47%. To propose the reaction mechanism in Fig. 2(a), vinylcyclobutane derivative from [2+2] cycloaddition was identified from GC-MS and NMR analysis and the rearrangement of the intermediate was also investigated. There are two distinct features of this photoredox system. The first is the role of dioxygen as electron mediator for photoinduced electrons, and it was emphasized several times. Because of this formation of radical species as an intermediate, this photoredox cycle becomes a radical-induced reaction, which is called as radical cation Diels-Alder cycloadditions. Next, in contrast to the existing Diels-Alder reaction, electronic states of substitutes around double bonds are irrelevant to the reaction progress, maintaining its enantio- and diastereoselectivity.

Another representative cycloaddition, [2+2] cycloaddition study was proceeded by CdSe QDs [75]. Contrary to other studies, Jones et al. focused on a theoretical mechanistic approach of 4-vinylbenzoic acid derivatives. Periodic and nonperiodic density functional theory (DFT) calculations are used to identify the origin of syn stereoselectivity via thermodynamic modeling of the surface on the CdSe QDs. Thermodynamic energies of each reaction step are determined, and the calculation derived the point that preferred binding of pairs through intermolecular reactions induce the reaction selectivity. Additionally, this study was generalized to other QDs, such as InSe or CdTe which have metal-enriched surfaces as that of CdSe.

With TiO_2 photocatalysis, both [2+2] and [4+2] cycloaddition reaction could be efficiently driven, following the mechanism in Fig. 2(b)-(c). Aromatic redox tag in [2+2] cycloaddition is well expressed in Fig. 2(c), which regulates both intermolecular and intramolecular SET processes. Variations of hexene, alkene, and aromatic redox tag were exhibited by a number of experiments. Also, cyclic voltammetry (CV) measurements and DFT calculations were used to propose reaction mechanism for the [2+2] cycloaddition. This photocatalysis has the advantages that the reaction is completed fast in less than 30 min, and does not need any sacrificial substrates.

Similar to g-C_3N_4, Nakayama et al. demonstrated TiO_2 photocatalysis to catalyze Diels-Alder reactions in $LiClO_4/CH_3NO_2$ solution

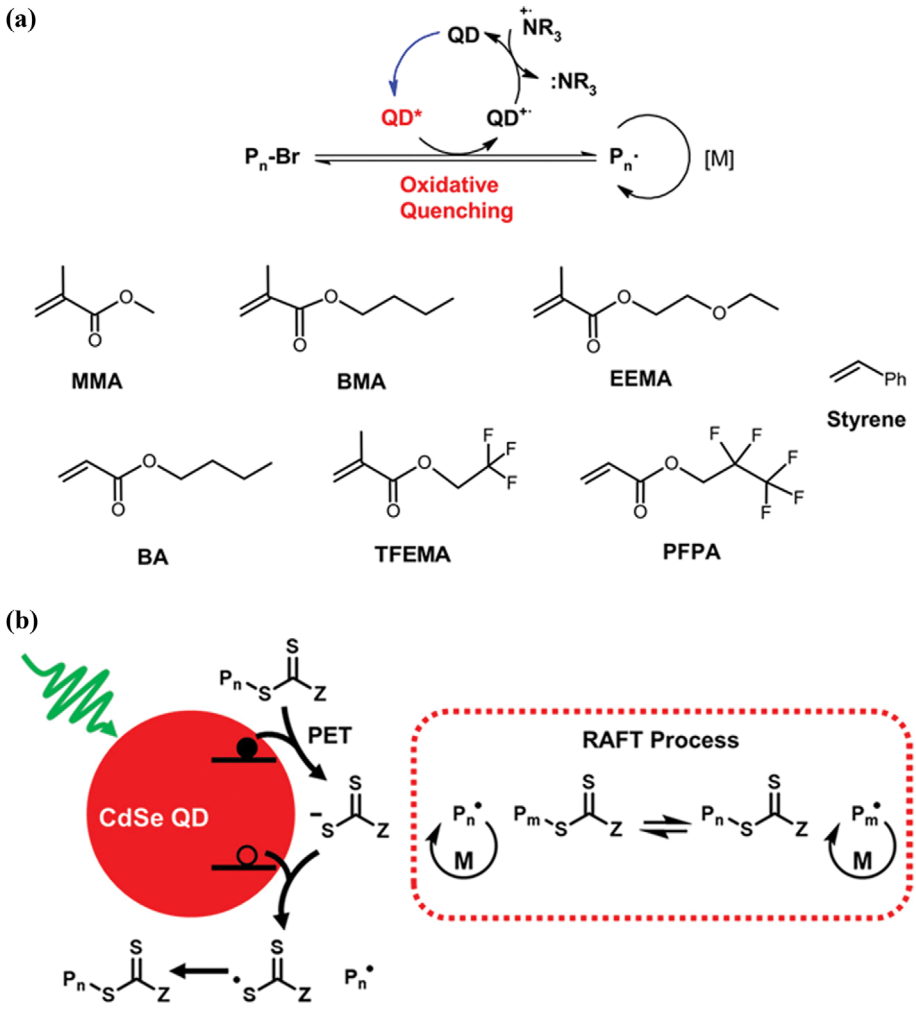

Fig. 3. (a) Schematic concept of oxidative quenching mechanism of light-mediated radical polymerization. Reproduced with permission from [77]. Copyright (2018) American Chemical Society. (b) Mechanism of photocatalyzed PET-RAFT polymerization catalyzed by CdSe QDs. Reproduced with permission from [42]. Copyright (2019) American Chemical Society.

[76]. Unlike other general Diels-Alder reactions, the combination of TiO_2 and $LiClO_4/CH_3NO_2$ can be a powerful redox option regardless of their nucleophilicity. The carbon nucleophiles and carbon-centered radical cations (formed at valence band) react first, and reduction reaction occurs at a conduction band to make a six-membered ring. It is proven that TiO_2 can efficiently drive [2+2] and [4+2] cycloaddition reaction both and is utilized as another useful tool in the field of synthetic organic chemistry.

1-3. Polymerization Reaction

Furthermore, distinctive photocatalytic polymerization processes which organize a great number of bonds were developed through CdSe QDs. Photoredox cycle with CdSe QDs in Fig. 3(a) was firstly used for atom transfer radical polymerization (ATRP) of (meth)acrylates, styrene, and construction of block copolymers [77]. In comparison with conventional molecular photoredox catalysts or expensive transition metals, the exceptional advantages of QD-based photocatalysts were emphasized again. Similarly, McClelland et al. have shown that MPA-capped CdSe QDs can be efficient and recyclable photocatalysts for photoinduced electron transfer reversible addition-fragmentation chain transfer (PET-RAFT) polymerization in Fig. 3(b) [42]. While the loading amount of molecular photocatalyst Eosin Y was 7.5 ppm, CdSe QDs were loaded only 0.43 ppm. In spite of low concentration of catalyst loading, extraordinary reaction rate and conversion efficiency were exhibited under identical reaction conditions. Additionally, the recyclability of catalysts was also shown by filtration experiments without significant decrease in efficiency.

2. Bond Cleavage Reaction

Bond cleavage reactions have been relatively less developed in comparison with bond formation reactions. Nevertheless, the study of bond cleavage has been receiving much attention these days, in the view of biomass conversion [36] or waste plastic conversion [78]. Lignocellulose, the most abundant form of biomass in earth, is composed of lignin, cellulose, and hemicellulose. Out of these, lignin and its model have been actively studied as accessible source of fine aromatic feedstocks [81-83]. In the lignin structure, C-C bond and C-O bond are rich in the main backbone, and for their bond cleavage the rate determining step is known as H-abstraction. Sequent reactions also occur by radical-induced mechanism like as previous reactions. Because of inertness of C-H bonds at initiation step, reaction seems to be challenging. However, high reaction rate and yield have been reported through heterogeneous catalysis and QD-based catalysis both.

2-1. Lignin Model Degradation

Lignin polymer backbone mainly includes C-C bonds and C-O bonds, and heterogenous semiconductor materials are credited for C-C bond cleavage. Prior to the entangled lignin polymer, a lignin model which has β-O-4 linkages was first studied. Selective and efficient photocatalytic C-C cleavage was achieved by vanadium oxo catalysts first [82]. As the strategy of photocatalytic oxidation protocol, C-C bond cleavage is driven by ligand-to-metal charge transfer (LMCT). By isotope labeling studies, two degradation products of the lignin model compounds were analyzed. Also, energy profiles of all intermediates and transients were theoretically calculated by DFT, and it confirmed that the reaction mechanism has low energy-barrier and exothermic pathways. This study is a unique and eco-friendly approach to perform selective C-C activation reaction under visible light (λ>420 nm) irradiation and with high yields.

Liu et al. reported that a selective carbon-carbon (C-C) decoupling reaction of lignin β-O-4 model can also be efficiently driven by g-C_3N_4 [35]. In contrast to vanadium oxo photocatalysis, the reaction is initiated by direct oxidation at valence band. They enhanced surface area of catalyst by mesoporous structure, increasing the efficiency. Increased surface area over four-times was measured by multipoint Brunauer-Emmett-Teller analysis. Mechanism of C-C bond cleavage is shown as Fig. 4(a). The conversion was up to 96%, and selectivity was 91%. The reason why conversion and selectivity were so high is explained by π-π stacking interaction between carbon nitride and aromatic substrates. Then, from elemental analysis, they argued that incomplete condensation induced the presence of hydrogen in g-C_3N_4 and it prevented electron-hole pair recombination. Additionally, DFT calculations supported this argument successfully. The application of carbon nitride photocatalysis was extended to not only C-C coupling but also C-C decoupling reaction.

In QD-based photocatalysis, cadmium chalcogenide QDs have

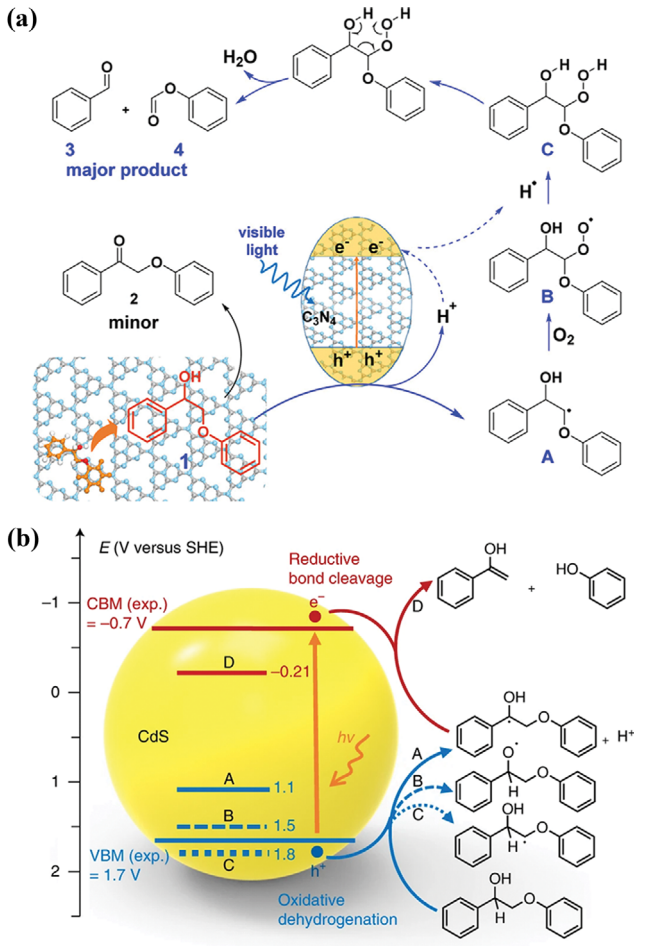

Fig. 4. (a) Mechanism of C-C bond cleavage of lignin β-O-4 model by graphitic carbon nitride. Reproduced with permission from [35]. Copyright (2020) American Chemical Society. (b) Scheme of C-O bond cleavage of lignin β-O-4 model by CdS QDs [36].

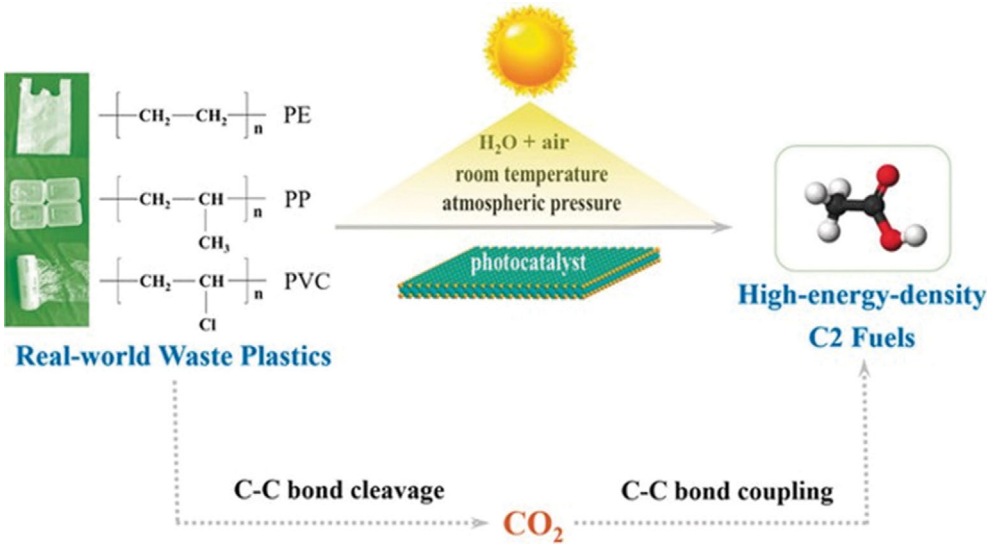

Fig. 5. Schematic illustration for photocatalytic conversion of waste plastics into C_2 fuels [78]. John Wiley & Sons. © 2020 WILEY-VCH Verlag GmbH & Co. KGaA, Weinheim.

shown outstanding activity for C-O bond cleavage. The final products are phenol and acetophenone compounds by C-O decoupling of lignin β-O-4 model, whereas C-C bond cleavage products are benzaldehyde and phenyl formate. Additionally, C_α radical is formed by H-abstraction in C-O bond cleavage mechanism. Enright et al. reported that CdSe QDs could catalyze C-O bond cleavage after oxidation of lignin β-O-4 model [83]. With equivalent catalyst loading as iridium catalysts, CdSe QDs exhibited 15 times greater turnover frequency. This study just focused on only the lignin model, not the polymeric biomass. But this progressive research can be expanded to the field of biomass depolymerization.

CdS QDs also exhibited fascinating solar energy-driven photocatalytic conversion compared to other heterogeneous catalysts [36]. The size of QDs (4.4 nm) and their ligands (3-mercaptopropionic acid, MPA) was optimized in the same condition. As shown in Fig. 4(b), the valence band potential (1.7 eV, vs. SHE) is appropriate to selective C-O bond cleavage, without C-C bond cleavage. The products of selective C-O bond cleavage were phenol and acetophenone, and their yield was over 90% with the CdS QDs which size was 4.4 nm. Surprisingly, after ten recycling experiments by a reversible aggregation-colloidization strategy, deactivation was not observed. The most noticeable point is that this research article covers not only lignin model, but also recyclable full utilization of lignocellulosic biomass. Aromatic monomers are produced by C-O bond cleavage of lignin, then xylose and glucose are formed by acidolysis and enzymolysis, sequentially. The experimental content of xylans and glucans reached to 90% and 98% in the original birch woodmeal, respectively. Also, control experiments with different additives or reactants proved the formation of α-carbon radical. Besides, mechanism for β-O-4 bond cleavage was proposed by several control experiments, such as scavenger addition or spin trapping reaction with 5-diisopropoxy-phosphoryl-5-methyl-1-pyrroline-N-oxide.

2-2. Plastic Degradation

Above all, recent study about conversion of waste plastics to C_2 fuels with niobium oxide (Nb_2O_5) layer photocatalysts has a big impact [78]. The overall scheme in Fig. 5 is organized as two main steps, C-C bond cleavage and C-C bond coupling. The reaction was reported under natural environment conditions, at room temperature and atmospheric pressure. Even though the specific mechanism of C-C bond cleavage was not identified, high selectivity and conversion of waste plastics were exhibited. PE, PP, and PVC were converted 100% into CO_2 within 40, 60, and 90 hours, respectively. The yield of CO_2-saturated system was measured for gas phase and solution phase both. The gas phase CO_2 was quantified by gas chromatograph, and dissolved CO_2 in aqueous solution was detected with precipitation method with $Ba(OH)_2$ powders. In addition, various methods such as in situ ESR spectra, synchrotron-radiation SVUV-PIMS spectra, UV-vis absorption spectra, and isotope-labeling experiments were used to demonstrate that dioxygen (O_2) and hydroxyl radical trigger the oxidative C-C cleavage. This two-step plastic-to-fuel conversion in natural environments may be helpful to solve the serious white pollution crisis. However, they mentioned that the current yield of C_2 fuels is still very low because of poor reduction activity of CO_2. Indeed, the evolution rate of CH_3COOH was more than 1,000 times lower than the CO_2 evolution rate. The anticipating point about simultaneous optimization of the respective C-C bond cleavage and bond-coupling processes was also emphasized.

3. Oxidation Reaction

Even though C-C decoupling includes oxidative bond cleavage and bond coupling, oxidation reactions without any changes in C-C bonds or C-O bonds are also developing fields. In particular, not only general oxidation reactions such as cyclohexane oxidation, but also photoreforming concepts to produce value-added products from biomass and waste plastics have been repeatedly proposed. Because oxidation reactions are driven by photo-generated holes, observation of holes and their efficient utilization are important.

In fact, simple oxidation reaction with TiO_2 photocatalysts such

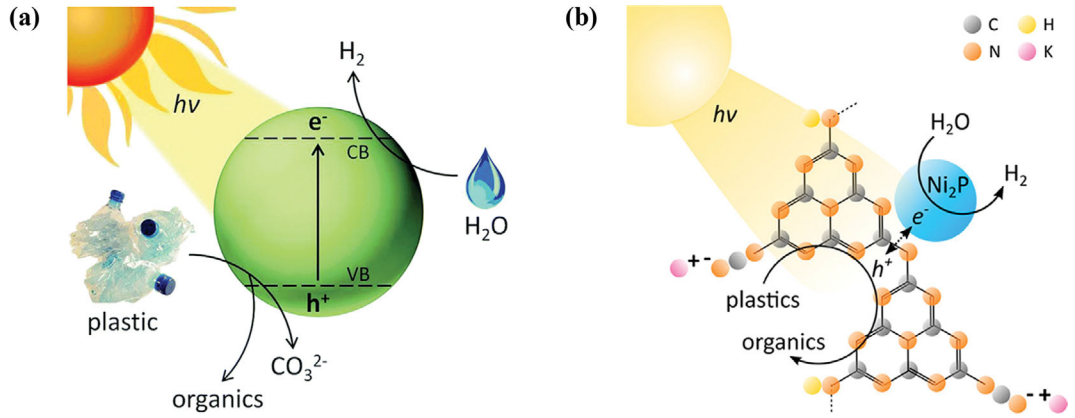

Fig. 6. (a) Diagram of solar-driven reforming of plastics waste to H_2 by CdS/CdOx. Reproduced from [92] with permission of The Royal Society of Chemistry. (b) Diagram of photoreforming of nonrecyclable plastic waste over CN_x|Ni_2P. Reproduced with permission from [93]. Copyright (2019) American Chemical Society.

as cyclohexane hydroxylation [84,85] or aromatics hydroxylation [89-91] is the conventional process. Mu et al. have studied the solvent effects for cyclohexane oxidation and achieved an 83% selectivity of cyclohexanone [85]. Then, hydroxylation of benzenes was reported by Fujihira et al., first with TiO_2-H_2O systems [86]. Fujihira et al. investigated various parameters such as pH, molecular oxygen, and Cu^{2+} ions for high selectivity. Yoshida et al. used platinum as cocatalyst for hydroxylation of benzenes, then the Pt/TiO_2 catalysts were used in water containing a high substrate concentration [88]. In the absence of molecular O_2, the reaction selectivity to phenol was greatly improved and protons were reacted as electron acceptors.

With CdS QDs, Wakerley et al. suggested a fancy photocatalytic concept about solar-driven lignocellulose reforming [89]. They produced H_2 fuel and oxidized valuable materials, using biomass. A pre-treatment and the reaction condition were aqueous NaOH solution. It is well known that the ester group can be hydrolyzed in acidic or alkaline condition [90,91], and lignocellulose do so. Thus, alkaline hydrolysis and subsequent oxidation reaction are the whole process of biomass valorization. The suitable band potential of CdS QDs enabled to reduce water to H_2 without any co-catalysts. Right after this study, the similar concept of plastic reforming was reported [92]. In this research, commonly produced polymers such as polyethylene terephthalate (PET), polylactic acid (PLA), and polyurethane (PUR) were used as feedstocks by the concept visualized in Fig. 6(a). Although both photoreforming mechanisms were not clearly defined, hydroxyl radicals are regarded as the key of oxidation. This hypothesis was also proven by scavenging experiments with terephthalic acid (TPA).

As well as, cadmium-free photoreforming of plastic (PET, PLA) was exhibited in study of Uekert et al. according to the scheme in Fig. 6(b) [93]. Potassium hydroxide (KOH) aqueous solution made PET and PLA into monomers by alkaline hydrolysis of their ester groups. Then, nickel phosphide (Ni_2P) cocatalyst assisted hydrogen production at conduction band, and hydrolyzed plastic monomers underwent direct oxidation by carbon nitride. This work is the first approach that used green and sustainable photocatalysis of plastic wastes as feedstock. And the products are hydrogen and valuable organic chemicals, such as formate and acetate. Furthermore, upscaling and real-world efficacy were evaluated through photoreforming of polyester microfibers and oil-contaminated PET. These solar-driven reforming concepts address two important challenge of plastic pollution and renewable H_2 generation simultaneously, and this has been developed to other precious studies [92-94].

CONCLUSIONS AND OUTLOOK

In conclusion, photocatalysis by semiconductor materials under visible light irradiation has extended to a wide branch of organic reactions, such as bond formation, bond cleavage, and oxidation. Many catalysts exhibit remarkable catalytic activity which is superior to conventional molecular photocatalysts. The vast majority of reactions have mechanism including reactive radical species: (1) hydroxyl radicals, (2) superoxide radicals, and (3) directly oxidized carbon radicals, leading to radical-induced transformation. Previously, many studies of photocatalytic organic transformation were limited to functional group transformation only. The absorption data of organic dye compounds usually identifies the small change of functional groups as a decomposition rate. However, in recent progressive studies, the specific intermediates and products were detected and their yield was also calculated.

Heterogeneous catalysts such as TiO_2 and g-C_3N_4 are proceeding green processes with practicable recycling, and catalysts with QDs usually exhibit high catalytic activity and reaction rate with small amount of catalyst loading. In sequence, recyclability of QD-based photocatalysts is even demonstrated, which has been challenging so far. Although inspiring environmental applications were reported, such as biomass conversion or plastic degradation, cadmium-based catalysis and its scalability matters still remain. For industrialization and real application, green and sustainable processes are inevitably required through heavy-metal free and harmless process.

Despite extensive research on photocatalysts by semiconductor materials, specific mechanism in organic transformation is not defined yet. Only few reaction intermediates have been detected by radical scavengers, and most mechanisms were just proposed with-

out any demonstration. Even though it is problematic because the reactions are induced by reactive radical intermediates which have short lifetime, identification will be beneficial for further application and development. Additionally, oxidation and hole are essential in most cases because radical intermediates are usually formed at valence band. Thus, the behavior of excitons should be more investigated as well as electrons for more comprehensive understanding.

ACKNOWLEDGEMENT

This work was funded by Saudi Aramco-KAIST CO_2 Management Center.

REFERENCES

1. H. K. Akira Fujishima, *Nature*, **238**, 38 (1972).
2. A. J. Esswein and D. G. Nocera, *Chem. Rev.*, **107**, 4022 (2007).
3. A. Kudo and Y. Miseki, *Chem. Soc. Rev.*, **38**, 253 (2009).
4. J. D. Holladay, J. Hu, D. L. King and Y. Wang, *Catal. Today*, **139**, 244 (2009).
5. K. Maeda and K. Domen, *J. Phys. Chem. Lett.*, **1**, 2655 (2010).
6. W. D. Kim, J. H. Kim, S. Lee, S. Lee, J. Y. Woo, K. Lee, W. S. Chae, S. Jeong, W. K. Bae, J. A. McGuire, J. H. Moon, M. S. Jeong and D. C. Lee, *Chem. Mater.*, **28**, 962 (2016).
7. K. Lee, C. H. Lee, J. Y. Cheong, S. Lee, I. D. Kim, H. I. Joh and D. C. Lee, *Korean J. Chem. Eng.*, **34**, 3214 (2017).
8. S. Chen, T. Takata and K. Domen, *Nat. Rev. Mater.*, **2**, 1 (2017).
9. T. Takata, J. Jiang, Y. Sakata, M. Nakabayashi, N. Shibata, V. Nandal, K. Seki, T. Hisatomi and K. Domen, *Nature*, **581**, 411 (2020).
10. J. Yu, J. Low, W. Xiao, P. Zhou and M. Jaroniec, *J. Am. Chem. Soc.*, **136**, 8839 (2014).
11. K. Wang, Q. Li, B. Liu, B. Cheng, W. Ho and J. Yu, *Appl. Catal. B Environ.*, **176-177**, 44 (2015).
12. H. Cho, W. D. Kim, K. Lee, S. Lee, G. S. Kang, H. I. Joh and D. C. Lee, *Appl. Surf. Sci.*, **429**, 2 (2018).
13. H. Cho, W. D. Kim, J. Yu, S. Lee and D. C. Lee, *ChemCatChem*, **10**, 5679 (2018).
14. S. Jeong, G. M. Kim, G. S. Kang, C. Kim, H. Lee, W. J. Kim, Y. K. Lee, S. Lee, H. Kim, H. K. Lim and D. C. Lee, *J. Phys. Chem. C*, **123**, 29184 (2019).
15. D. Li, H. Haneda, S. Hishita and N. Ohashi, *Chem. Mater.*, **17**, 2596 (2005).
16. J. Mo, Y. Zhang, Q. Xu, J. J. Lamson and R. Zhao, *Atmos. Environ.*, **43**, 2229 (2009).
17. T. Ochiai and A. Fujishima, *J. Photochem. Photobiol. C Photochem. Rev.*, **13**, 247 (2012).
18. I. Ghosh, L. Marzo, A. Das, R. Shaikh and B. König, *Acc. Chem. Res.*, **49**, 1566 (2016).
19. S. Lin, M. A. Ischay, C. G. Fry and T. P. Yoon, *J. Am. Chem. Soc.*, **133**, 19350 (2011).
20. M. A. Cismesia and T. P. Yoon, *Chem. Sci.*, **6**, 5426 (2015).
21. S. N. Ahmed and W. Haider, *Nanotechnology*, **29**, 342001 (2018).
22. C. Huang, J. Wen, Y. Shen, F. He, L. Mi, Z. Gan, J. Ma, S. Liu, H. Ma and Y. Zhang, *Chem. Sci.*, **9**, 7912 (2018).
23. T. Adachi, S. S. Latthe, S. W. Gosavi, N. Roy, N. Suzuki, H. Ikari, K. Kato, K. Katsumata, K. Nakata, M. Furudate, T. Inoue, T. Kondo, M. Yuasa, A. Fujishima and C. Terashima, *Appl. Surf. Sci.*, **458**, 917 (2018).
24. J. Zhang, X. Chen, K. Takanabe, K. Maeda, K. Domen, J. D. Epping, X. Fu, M. Antonieta and X. Wang, *Angew. Chem. - Int. Ed.*, **49**, 441 (2010).
25. J. Zhu, P. Xiao, H. Li and S. A. C. Carabineiro, *ACS Appl. Mater. Interfaces*, **6**, 16449 (2014).
26. Z. Zhang, K. Edme, S. Lian and E. A. Weiss, *J. Am. Chem. Soc.*, **139**, 4246 (2017).
27. J. A. Caputo, L. C. Frenette, N. Zhao, K. L. Sowers, T. D. Krauss and D. J. Weix, *J. Am. Chem. Soc.*, **139**, 4250 (2017).
28. J. M. Caruge, J. E. Halpert, V. Wood, V. Buloví and M. G. Bawendi, *Nat. Photonics.*, **2**, 247 (2008).
29. V. Wood and V. Bulović, *Nano Rev.*, **1**, 5202 (2010).
30. Y. F. Xu, M. Z. Yang, B. X. Chen, X. D. Wang, H. Y. Chen, D. B. Kuang and C. Y. Su, *J. Am. Chem. Soc.*, **139**, 5660 (2017).
31. L. Ge, F. Zuo, J. Liu, Q. Ma, C. Wang, D. Sun, L. Bartels and P. Feng, *J. Phys. Chem. C*, **116**, 13708 (2012).
32. F. T. Rabouw and C. de Mello Donega, *Top. Curr. Chem.*, **374**, (2016).
33. H. Lee, D. E. Yoon, S. Koh, M. S. Kang, J. Lim and D. C. Lee, *Chem. Sci.*, **11**, 2318 (2020).
34. D. Kim and D. C. Lee, *J. Phys. Chem. Lett.*, **11**, 2647 (2020).
35. H. Liu, H. Li, J. Lu, S. Zeng, M. Wang, N. Luo, S. Xu and F. Wang, *ACS Catal.*, **8**, 4761 (2018).
36. X. Wu, X. Fan, S. Xie, J. Lin, J. Cheng, Q. Zhang, L. Chen and Y. Wang, *Nat. Catal.*, **1**, 772 (2018).
37. L. Yin and J. Liebscher, *Chem. Rev.*, **107**, 133 (2007).
38. C. S. Yeung and V. M. Dong, *Chem. Rev.*, **111**, 1215 (2011).
39. N. Miyaura, K. Yamada and A. Suzuki, *Tetrahedron Lett.*, **20**, 3437 (1979).
40. J. Zoller, D. C. Fabry and M. Rueping, *ACS Catal.*, **5**, 3900 (2015).
41. Y. Zhao and M. Antonietti, *Angew. Chem.*, **129**, 9464 (2017).
42. K. P. McClelland, T. D. Clemons, S. I. Stupp and E. A. Weiss, *ACS Macro Lett.*, **9**, 7 (2020).
43. S. K. Kuriechen, S. Murugesan and S. P. Raj, *J. Catal.*, **2013**, 1 (2013).
44. T. Hirakawa, K. Yawata and Y. Nosaka, *Appl. Catal. A Gen.*, **325**, 105 (2007).
45. I. K. Konstantinou and T. A. Albanis, *Appl. Catal. B Environ.*, **49**, 1 (2004).
46. M. Auffan, M. Pedeutour, J. Rose, A. Masion, F. Ziarelli, D. Borschneck, C. Chaneac, C. Botta, P. Chaurand, J. Labille and J. Y. Bottero, *Environ. Sci. Technol.*, **44**, 2689 (2010).
47. Y. Li, L. Tang, S. Peng, Z. Li and G. Lu, *CrystEngComm*, **14**, 6974 (2012).
48. H. Park, H. H. Ou, U. Kang, J. Choi and M. R. Hoffmann, *Catal. Today*, **266**, 153 (2016).
49. T. Mitkina, C. Stanglmair, W. Setzer, M. Gruber, H. Kisch and B. König, *Org. Biomol. Chem.*, **10**, 3556 (2012).
50. S. C. Jensen, S. B. Homan and E. A. Weiss, *J. Am. Chem. Soc.*, **138**, 1591 (2016).
51. S. Lian, J. A. Christensen, M. S. Kodaimati, C. R. Rogers, M. R. Wasielewski and E. A. Weiss, *J. Phys. Chem. C*, **123**, 5923 (2019).
52. T. H. Thanh, D. H. Thanh and V. Q. Lam, *Adv. Optoelectron.*, **2014**, 9 (2014).

53. L. Cheng, Q. Xiang, Y. Liao and H. Zhang, *Energy Environ. Sci.*, **11**, 1362 (2018).
54. A. Noble and D. W. C. MacMillan, *J. Am. Chem. Soc.*, **136**, 11602 (2014).
55. D. Kim, Y. K. Lee, D. Lee, W. D. Kim, W. K. Bae and D. C. Lee, *ACS Nano*, **11**, 12461 (2017).
56. D. E. Yoon, W. D. Kim, D. Kim, D. Lee, S. Koh, W. K. Bae and D. C. Lee, *J. Phys. Chem. C*, **121**, 24837 (2017).
57. W. D. Kim, D. E. Yoon, D. Kim, S. Koh, W. K. Bae, W. S. Chae and D. C. Lee, *J. Phys. Chem. C*, **123**, 9445 (2019).
58. C. Harris and P. V. Kamat, *ACS Nano*, **4**, 7321 (2010).
59. C. Ma, D. Wu, X. Yao, X. Liu, M. Wei, Y. Liu, Z. Ma, P. Huo and Y. Yan, *J. Alloys Compd.*, **712**, 486 (2017).
60. W. Xia, J. Wu, J. C. Hu, S. Sun, M. De Li, H. Liu, M. Lan and F. Wang, *ChemSusChem*, **12**, 4617 (2019).
61. I. N. Chakraborty, S. Roy, G. Devatha, A. Rao and P. P. Pillai, *Chem. Mater.*, **31**, 2258 (2019).
62. S. Koh, T. Eom, W. D. Kim, K. Lee, D. Lee, Y. K. Lee, H. Kim, W. K. Bae and D. C. Lee, *Chem. Mater.*, **29**, 6346 (2017).
63. D. Lee, S. Koh, D. E. Yoon, S. Lee, W. D. Kim, D. Kim, W. K. Bae, J. Lim and D. C. Lee, *Korean J. Chem. Eng.*, **36**, 1518 (2019).
64. S. Koh, H. Lee, T. Lee, K. Park, W. J. Kim and D. C. Lee, *J. Chem. Phys.*, **151**, 144704 (2019).
65. W. D. Kim, D. Kim, D. E. Yoon, H. Lee, J. Lim, W. K. Bae and D. C. Lee, *Chem. Mater.*, **31**, 3066 (2019).
66. L. Li and P. Reiss, *J. Am. Chem. Soc.*, **130**, 11588 (2008).
67. J. G. Martin and R. K. Hill, *Chem. Rev.*, **61**, 537 (1961).
68. X. Jiang and R. Wang, *Chem. Rev.*, **113**, 5515 (2013).
69. Y. Guo, T. Chen, Q. Liu, Z. Zhang and X. Fang, *J. Phys. Chem. C*, **120**, 25328 (2016).
70. G. Zhang, Z. A. Lan, L. Lin, S. Lin and X. Wang, *Chem. Sci.*, **7**, 3062 (2016).
71. X. Wang, S. Blechert and M. Antonietti, *ACS Catal.*, **2**, 1596 (2012).
72. Y. Kang, Y. Yang, L. C. Yin, X. Kang, G. Liu and H. M. Cheng, *Adv. Mater.*, **27**, 4572 (2015).
73. J. Zhu, P. Xiao, H. Li and S. A. C. Carabineiro, *ACS Appl. Mater. Interfaces*, **6**, 16449 (2014).
74. S. Hu, F. Li, Z. Fan, F. Wang, Y. Zhao and Z. Lv, *Dalt. Trans.*, **44**, 1084 (2014).
75. L. O. Jones, M. A. Mosquera, Y. Jiang, E. A. Weiss, G. C. Schatz and M. A. Ratner, *J. Am. Chem. Soc.*, **142**, 15488 (2020).
76. K. Nakayama, N. Maeta, G. Horiguchi, H. Kamiya and Y. Okada, *Org. Lett.*, **21**, 2246 (2019).
77. Y. Huang, Y. Zhu and E. Egap, *ACS Macro Lett.*, **7**, 184 (2018).
78. X. Jiao, K. Zheng, Q. Chen, X. Li, Y. Li, W. Shao, J. Xu, J. Zhu, Y. Pan, Y. Sun and Y. Xie, *Angew. Chem. - Int. Ed.*, **59**, 15497 (2020).
79. G. Han, T. Yan, W. Zhang, Y. C. Zhang, D. Y. Lee, Z. Cao and Y. Sun, *ACS Catal.*, **9**, 11341 (2019).
80. Y. Gao, J. Zhang, X. Chen, D. Ma and N. Yan, *Chempluschem*, **79**, 825 (2014).
81. Y. T. Tsai, C. Y. Chen, Y. J. Hsieh and M. L. Tsai, *Eur. J. Inorg. Chem.*, **2019**, 4637 (2019).
82. S. Gazi, W. K. H. Ng, R. Ganguly, A. M. P. Moeljadi, H. Hirao and H. S. Soo, *Chem. Sci.*, **6**, 7130 (2015).
83. M. J. Enright, K. Gilbert-Bass, H. Sarsito and B. M. Cossairt, *Chem. Mater.*, **31**, 2677 (2019).
84. W. Mu, J. M. Herrmann and P. Pichat, *Catal. Lett.*, **3**, 73 (1989).
85. C. B. Almquist and P. Biswas, *Appl. Catal. A Gen.*, **214**, 259 (2001).
86. M. Fujihira, Y. Satoh and T. Osa, *Nature*, **293**, 206 (1981).
87. T. Ohno, K. Tokieda, S. Higashida and M. Matsumura, *Appl. Catal. A Gen.*, **244**, 383 (2003).
88. H. Yoshida, H. Yuzawa, M. Aoki, K. Otake, H. Itoh and T. Hattori, *Chem. Commun.*, 4634 (2008).
89. D. W. Wakerley, M. F. Kuehnel, K. L. Orchard, K. H. Ly, T. E. Rosser and E. Reisner, *Nat. Energy*, **2**, 1 (2017).
90. M. Charton, *J. Am. Chem. Soc.*, **97**, 3691 (1975).
91. D. Stefanidis and W. P. Jencks, *J. Am. Chem. Soc.*, **115**, 6045 (1993).
92. T. Uekert, M. F. Kuehnel, D. W. Wakerley and E. Reisner, *Energy Environ. Sci.*, **11**, 2853 (2018).
93. T. Uekert, H. Kasap and E. Reisner, *J. Am. Chem. Soc.*, **141**, 15201 (2019).
94. T. Uekert, F. Dorchies, C. M. Pichler and E. Reisner, *Green Chem.*, **22**, 3262 (2020).
95. D. S. Achilleos, W. Yang, H. Kasap, A. Savateev, Y. Markushyna, J. R. Durrant and E. Reisner, *Angew. Chem. - Int. Ed.*, **59**, 18184 (2020).
96. C. M. Pichler, T. Uekert and E. Reisner, *Chem. Commun.*, **56**, 5743 (2020).
97. Y. Okada, N. Maeta, K. Nakayama and H. Kamiya, *J. Org. Chem.*, **83**, 4948 (2018).

Doh C. Lee is a professor in the Department of Chemical and Biomolecular Engineering at KAIST. He joined KAIST in 2010 after working at Los Alamos National Laboratory for three years as a director's postdoctoral fellow. Dr. Lee served as General Secretary at the 9th International Conference on Quantum Dots (QD2016) and he has been on the International Advisory Committee for QD2018 and QD2020.